Singular variation property of elastic constants of piezoelectric ceramics shunted to negative capacitance

Ji-Ying Hu(胡吉英)[1], Zhao-Hui Li(李朝晖)[1,†], and Qi-Hu Li(李启虎)[2]

[1] *Department of Electronics, Peking University, Beijing* 100871, *China*
[2] *Advanced Technology Institute, Peking University, Beijing* 100871, *China*

(Received 19 July 2017; revised manuscript received 11 September 2017; published online 20 November 2017)

Piezoelectric shunt damping has been widely used in vibration suppression, sound absorption, noise elimination, etc. In such applications, the variant elastic constants of piezoelectric materials are the essential parameters that determine the performances of the systems, when piezoelectric materials are shunted to normal electrical elements, i.e., resistance, inductance and capacitance, as well as their combinations. In recent years, many researches have demonstrated that the wideband sound absorption or vibration suppression can be realized with piezoelectric materials shunted to negative capacitance. However, most systems using the negative-capacitance shunt circuits show their instabilities in the optimal condition, which are essentially caused by the singular variation properties of elastic constants of piezoelectric materials when shunted to negative capacitance. This paper aims at investigating the effects of negative-capacitance shunt circuits on elastic constants of a piezoelectric ceramic plate through theoretical analyses and experiments, which gives an rational explanation for why negative capacitance shunt circuit is prone to make structure instable. First, the relationships between the elastic constants c_{11}, c_{33}, c_{55} of the piezoelectric ceramic and the shunt negative capacitance are derived with the piezoelectric constitutive law theoretically. Then, an experimental setup is established to verify the theoretical results through observing the change of elastic constant c_{55} of the shunted piezoelectric plate with the variation of negative capacitance. The experimental results are in good agreement with the theoretical analyses, which reveals that the instability of the shunt damping system is essentially caused by the singular variation property of the elastic constants of piezoelectric material shunted to negative capacitance.

Keywords: piezoelectric ceramics, elastic constant, shunt damping, negative capacitance

PACS: 77.90.+k, 62.20.–x, 62.20.de, 81.40.Jj **DOI:** 10.1088/1674-1056/26/12/127702

1. Introduction

The piezoelectric shunt damping used in vibration suppression,[1–4] sound absorption,[5–8] noise elimination,[9,10] as well as wave propagation control[11] has been widely studied in the past few years. Because piezoelectric materials take the role in converting the mechanical vibration energy into electrical energy which is dissipated through passive circuits, shunt damping is also referred to as the semi-active technology.[5]

Resistance and inductance (RL) shunt circuits, connecting in series or parallel, are the first proposed efficient circuits for piezoelectric shunt damping[1,2] to suppress single mode vibration. Successively, multiple modes damping with resistance, inductance and capacitance (RLC) branches have been investigated.[12–14] However, there are a number of problems associated with these circuits, of which the foremost ones are the complexity and size of the circuit required to implement the total impedance. Typically, the shunt circuits for low frequency applications need large inductance values up to 1000 s of Henries, therefore Riordan gyrators[15] are required to implement the inductor elements, which are large in size and sensitive to component tolerances. Besides, the effectiveness of the systems with RL shunt circuits is generally limited to a narrow frequency range around each resonant frequency.

In recent years, the negative capacitance technique used in piezoelectric shunt damping has been proved to be able to improve the bandwidth performance of vibration suppression.[16,17] The effect of negative capacitance is to cancel out the inherent capacitive impedance of the piezoelectric material and maximize the energy dissipation in a resistor, with which the wideband matching condition is realized and multiple modes are suppressed. For example, Behrens *et al.*[17] adopted the negative capacitance in series with a resistance to suppress the vibration of clamped beam , through which the resonant amplitudes of the first five modes are reduced by 6.1, 16.3, 15.2, 11.7, and 10.2 dB experimentally. As a negative capacitance circuit can affect the elasticity of the piezoelectric ceramic, piezoelectric shunt damping techniques are also applied to sound absorption.[18,19] Fukada *et al.* showed the efficiency improvement of a negative capacitance circuit connected to a curved PVDF film in sound isolation application.[18] Changing the elasticity of the piezo film, the overall transmission loss level of 40 dB was achieved. Yu *et al.* also demonstrated that a negative capacitance combining with a proper resistance can achieve wideband sound absorption performance.[19]

†Corresponding author. E-mail: lizhcat@pku.edu.cn

© 2017 Chinese Physical Society and IOP Publishing Ltd

Although negative capacitance shunt circuits have the above advantages when applied to sound absorption or vibration suppression systems, they may bring instability problems to the structures if improperly tuned.[20,21] Han *et al.* proved that the highest performance of vibration suppression is reached when the external capacitance approaches to the negative value of the inner piezoelectric capacitance, which is just the stability boundary of the system.[22] Neubauer and Wallaschek pointed out that the negative capacitance is essentially an active circuit that can destabilize the structure if it is improperly tuned.[23] They also analyzed and derived the stability condition specifically in view of energy consumption.

Among the above-mentioned applications, the piezoelectric materials shunted to negative capacitance mainly working in one of three modes: the transverse mode, the longitudinal mode and the shear mode.[2] Elastic constants c_{11}, c_{33}, and c_{55} of piezoelectric materials corresponding to the above three modes are the essential parameters which determine the performances of the vibration suppression and sound absorption systems. In fact, the singular variation properties of elastic constants with shunt negative capacitance are the inner reason for the instabilities of shunt damping systems. So it is of great research value to investigate the relationships between the elastic constants and the shunt negative capacitance, which is also a foundation to solve the instability problem when designing vibration suppression and sound absorption systems by using piezoelectric materials shunted to negative capacitance. Thus in this paper, first, the piezoelectric constitutive equations are used to derived the relationships between the elastic constants c_{11}, c_{33}, c_{55} and the negative capacitance respectively. Then, the theoretical results are verified through experimental observations. Taking the test of the elastic constant c_{55} for example, an experimental setup is established to test the influence of negative capacitance on c_{55} indirectly.[24]

The rest of this paper is organized as follows. In Section 2 analyzed are the relationships between the elastic constants of piezoelectric materials and the shunt negative capacitance theoretically with piezoelectric constitutive equations. In Section 3, the experiment setup and the experimental results are presented. In Section 4, the inner reason why the negative circuit is prone to make systems unstable is discussed. Finally, some conclusions are drawn in Section 5.

2. Theoretical analyses

In this section the influence of negative capacitance on elastic constants of piezoelectric materials theoretically is analyzed. It reveals that the singular variation properties of elastic constants of the piezoelectric materials are the inner cause of the instability of system shunted to negative capacitance.

2.1. Stability boundary of the shunt damping system with shunted negative capacitance.

In Ref. [20], Neubauer *et al.* employed a thickness-mode mechanical resonator as shown in Fig. 1, to derive the negative capacitance range which makes the system unstable from the view of resonance frequency of the structure. The range of negative capacitance is derived as

$$-1 < \frac{C_{\mathrm{p}}}{C} < -\frac{1}{1+\gamma}, \tag{1}$$

$$\gamma = \frac{(k_1 d_{33})^2}{C_{\mathrm{p}}(k_0 + k_1)}, \tag{2}$$

where C_{p} is the inner capacitance of the piezoelectric element under a constant strain, C is the value of negative capacitance, d_{33} is the charge density per unity stress under a constant electric field, and $k_1 = c_{33}(A_{\mathrm{p}}/l_{\mathrm{p}})$ is the mechanical stiffness of the piezoelectric material, with c_{33} being the elastic constant of thickness mode. If the mechanical spring-damper (k_0, d_0) in the model in Fig. 1 is omitted, with k_0 and d_0 being the stiffness and the damping coefficient respectively, γ is simplified into

$$\gamma = \frac{(k_1 d_{33})^2}{C_{\mathrm{p}} k_1} = k_{33}^2, \tag{3}$$

where k_{33} is electromechanical coupling coefficient.

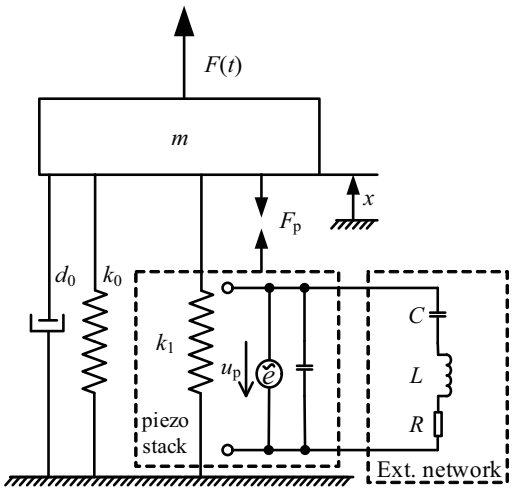


Fig. 1. Mechanical model with piezoelectric element connected to external LRC-network cited from Ref. [20].

Then the range of negative capacitance making the system unstable is obtained to be

$$-\left(1+k_{33}^2\right) C_{\mathrm{p}} < C < -C_{\mathrm{p}}. \tag{4}$$

Inequality (4) gives the unstable range of the shunted negative capacitance, but without giving a rational explanation. In fact, when the value of shunt negative capacitance is in a specific range, the elastic constant is lower than zero, which is not meaningful as shown in latter parts of this paper.

2.2. Influences of negative capacitance on elastic constants of the piezoelectric materials

The diagram of a piezoelectric plate shunted to a negative capacitor is shown in Fig. 2(a), which may work in three modes: the transverse mode, the longitudinal mode and the shear mode. At low frequency, the piezoelectric plate is usually modeled as a capacitor $C_{\rm p}$ in series with a voltage source $V_{\rm p}$. The equivalent circuit of the model can be depicted in Fig. 2(b), in which the function of the negative capacitor is mainly to counteract the inner capacitance $C_{\rm p}$ of the piezoelectric plate. Obviously, it has the advantage of simple implementation when acting as a multiple-mode vibration controller or broadband sound absorber.

Denote $\boldsymbol{V}$ and $\boldsymbol{I}$ as the voltage and current arrays, i.e., use V_i and I_i ($i=1, 2, 3$) to represent the voltages and currents when electrodes are in three directions respectively. According to the basic electrical circuit, the relationships between voltage $\boldsymbol{V}$ and electric field $\boldsymbol{E}$, and between current $\boldsymbol{I}$ and electric displacement $\boldsymbol{D}$ in the Laplace domain can be written as

$$\boldsymbol{V}(s)=\boldsymbol{L}\cdot\boldsymbol{E}(s), \tag{5a}$$

$$\boldsymbol{I}(s)=s\boldsymbol{A}\cdot\boldsymbol{D}(s), \tag{5b}$$

where $\boldsymbol{L}$ is a diagonal matrix of the length of the piezoelectric plate, and L_i ($i=1, 2, 3$) denotes the length in the ith direction. $\boldsymbol{A}$ is the diagonal matrix of the area of surface, and A_i ($i=1, 2, 3$) denotes the area perpendicular to the i-th direction, and s is the Laplace transform variable. Their forms are as follows:

$$\boldsymbol{V}=\begin{bmatrix}V_1\\V_2\\V_3\end{bmatrix},\quad \boldsymbol{I}=\begin{bmatrix}I_1\\I_2\\I_3\end{bmatrix},\quad \boldsymbol{E}=\begin{bmatrix}E_1\\E_2\\E_3\end{bmatrix},\quad \boldsymbol{D}=\begin{bmatrix}D_1\\D_2\\D_3\end{bmatrix},$$

$$\boldsymbol{A}=\begin{bmatrix}A_1&0&0\\0&A_2&0\\0&0&A_3\end{bmatrix},\quad \boldsymbol{L}=\begin{bmatrix}L_1&0&0\\0&L_2&0\\0&0&L_3\end{bmatrix}.$$

The $\boldsymbol{e}$-type piezoelectric constitutive law is convenient in this case, which can be written from Ref. [25] as

$$\boldsymbol{D}=\varepsilon^{\rm S}\boldsymbol{E}+\boldsymbol{e}\boldsymbol{S}, \tag{6a}$$

$$\boldsymbol{T}=-\tilde{\boldsymbol{e}}\boldsymbol{E}+\boldsymbol{c}^{\rm E}\boldsymbol{S}, \tag{6b}$$

where $\boldsymbol{T}$ is the vector expression of the mechanical stress tensor, T_h ($h=1, 2, 3, 4, 5, 6$), and $\boldsymbol{S}$ is that of the mechanical strain tensor, S_h ($h=1, 2, 3, 4, 5, 6$). The matrix $\boldsymbol{e}$ denotes the piezoelectric stress coupling matrix, $\tilde{\boldsymbol{e}}$ is the transposed matrix of $\boldsymbol{e}$, $c^{\rm E}$ is the elastic constant matrix at a constant electric field, and $\varepsilon^{\rm S}$ is the permittivity matrix under a constant strain. The element forms of the above tensors and matrixes are referred to Ref. [25], which are written as follows:

$$\boldsymbol{S}=\begin{bmatrix}S_1\\S_2\\S_3\\S_4\\S_5\\S_6\end{bmatrix},\quad \boldsymbol{T}=\begin{bmatrix}T_1\\T_2\\T_3\\T_4\\T_5\\T_6\end{bmatrix},$$

$$\boldsymbol{c}^{\rm E}=\begin{bmatrix}c_{11}^{\rm E}&c_{12}^{\rm E}&c_{13}^{\rm E}&0&0&0\\c_{12}^{\rm E}&c_{11}^{\rm E}&c_{13}^{\rm E}&0&0&0\\c_{13}^{\rm E}&c_{13}^{\rm E}&c_{33}^{\rm E}&0&0&0\\0&0&0&c_{55}^{\rm E}&0&0\\0&0&0&0&c_{55}^{\rm E}&0\\0&0&0&0&0&c_{66}^{\rm E}\end{bmatrix},$$

$$\varepsilon^{\rm S}=\begin{bmatrix}\varepsilon_1^{\rm S}&0&0\\0&\varepsilon_1^{\rm S}&0\\0&0&\varepsilon_3^{\rm S}\end{bmatrix},$$

$$\boldsymbol{e}=\begin{bmatrix}0&0&0&0&d_{15}&0\\0&0&0&d_{15}&0&0\\d_{31}&d_{31}&d_{33}&0&0&0\end{bmatrix}.$$

Combining Eqs. (5) and Eqs. (6), the piezoelectric constitutive equations in terms of the current and the voltage can be written as:

$$\boldsymbol{I}=s\boldsymbol{A}\varepsilon^{\rm S}\boldsymbol{L}^{-1}\boldsymbol{V}+s\boldsymbol{A}\boldsymbol{e}\boldsymbol{S}, \tag{7a}$$

$$\boldsymbol{T}=-\tilde{\boldsymbol{e}}\boldsymbol{L}^{-1}\boldsymbol{V}+\boldsymbol{c}^{\rm E}\boldsymbol{S}. \tag{7b}$$

With the inner capacitance of the piezoelectric plate under a constant strain expressed as

$$\boldsymbol{C}_{\rm p}^{\rm S}=\boldsymbol{A}\varepsilon^{\rm S}\boldsymbol{L}^{-1}, \tag{8}$$

equation (7a) can be simplified into

$$\boldsymbol{I}=s\boldsymbol{C}_{\rm p}^{\rm S}\boldsymbol{V}+s\boldsymbol{A}\boldsymbol{e}\boldsymbol{S}=\boldsymbol{Y}^{\rm D}(s)\boldsymbol{V}+s\boldsymbol{A}\boldsymbol{e}\boldsymbol{S}, \tag{9}$$

where $\boldsymbol{Y}^{\rm D}(s)$ is the admittance matrix of the piezoelectric plate in an open-circuit state. When the piezoelectric plate is shunted to a negative capacitor as shown in Fig. 2, the admittances of the shunted piezoelectric plate in three directions, denoted by a diagonal matrix $Y^{\rm SH}$, can be obtained to be

$$\boldsymbol{Y}^{\rm SH}=s(\boldsymbol{C}_{\rm p}^{\rm S}-\boldsymbol{C}_x), \tag{10}$$

where

$$\boldsymbol{Y}^{\rm SH}(s)=\begin{bmatrix}Y_1^{\rm SH}(s)&0&0\\0&Y_2^{\rm SH}(s)&0\\0&0&Y_3^{\rm SH}(s)\end{bmatrix},$$

$$\boldsymbol{C}_{\rm p}^{\rm S}=\begin{bmatrix}C_{\rm p1}^{\rm S}&0&0\\0&C_{\rm p2}^{\rm S}&0\\0&0&C_{\rm p3}^{\rm S}\end{bmatrix},$$

$$\boldsymbol{C}_x^{=}\begin{bmatrix}C_{x1}&0&0\\0&C_{x2}&0\\0&0&C_{x3}\end{bmatrix}.$$

So the governing constitutive equation for a piezoelectric plate is

$$\boldsymbol{I} = \boldsymbol{Y}^{\mathrm{SH}}\boldsymbol{V} + s\boldsymbol{A}\boldsymbol{e}\boldsymbol{S} = s\left(\boldsymbol{C}_{\mathrm{p}}^{\mathrm{S}} - \boldsymbol{C}_x\right)\boldsymbol{V} + s\boldsymbol{A}\boldsymbol{e}\boldsymbol{S}. \tag{11}$$

From Eq. (11), the voltage is obtained to be

$$\boldsymbol{V} = \boldsymbol{Z}^{\mathrm{SH}}(\boldsymbol{I} - s\boldsymbol{A}\boldsymbol{e}\boldsymbol{S}), \tag{12}$$

where $\boldsymbol{Z}^{\mathrm{SH}} = (\boldsymbol{Y}^{\mathrm{SH}})^{-1} = (\boldsymbol{C}_{\mathrm{p}}^{\mathrm{S}} - \boldsymbol{C}_x)^{-1}/s$ is the impedance of a piezoelectric plate shunted to a negative capacitor. By inserting Eq. (12) into Eq. (7b), the stress tensor can be obtained as follows:

$$\boldsymbol{T} = \left(\boldsymbol{c}^{\mathrm{E}} + \tilde{\boldsymbol{e}}\boldsymbol{L}^{-1}\boldsymbol{Z}^{\mathrm{SH}}s\boldsymbol{A}\boldsymbol{e}\right)\boldsymbol{S} - \tilde{\boldsymbol{e}}\boldsymbol{L}^{-1}\boldsymbol{Z}^{\mathrm{SH}}\boldsymbol{I}. \tag{13}$$

The elastic constant array of the shunt piezoelectric plate under constant electric displacement, i.e. constant $\boldsymbol{I}$, can be defined from Eq. (13) as

$$\begin{aligned}\boldsymbol{c}^{\mathrm{SH}} &= \boldsymbol{c}^{\mathrm{E}} + \tilde{\boldsymbol{e}}\boldsymbol{L}^{-1}\boldsymbol{Z}^{\mathrm{SH}}s\boldsymbol{A}\boldsymbol{e} \\ &= \boldsymbol{c}^{\mathrm{E}} + \tilde{\boldsymbol{e}}\boldsymbol{C}_{\mathrm{p}}^{\mathrm{S}}\boldsymbol{e}(\boldsymbol{C}_{\mathrm{p}}^{\mathrm{S}} - \boldsymbol{C}_x)^{-1}(\boldsymbol{\varepsilon}^{\mathrm{S}})^{-1}.\end{aligned} \tag{14}$$

By defining the non-dimensional electrical impedance

$$\boldsymbol{\eta}^{\mathrm{SH}} = \boldsymbol{Z}^{\mathrm{SH}}(\boldsymbol{Z}^{\mathrm{D}})^{-1} = \boldsymbol{C}_{\mathrm{p}}^{\mathrm{S}}(\boldsymbol{C}_{\mathrm{p}}^{\mathrm{S}} - \boldsymbol{C}_x)^{-1}, \tag{15}$$

equation (16) can be simplified into

$$\boldsymbol{c}^{\mathrm{SH}} = \boldsymbol{c}^{\mathrm{E}} + \tilde{\boldsymbol{e}}\boldsymbol{\eta}^{\mathrm{SH}}(\boldsymbol{\varepsilon}^{\mathrm{S}})^{-1}\boldsymbol{e}. \tag{16}$$

As the shunted piezoelectric plate usually works in one of three modes: the transverse mode, the longitudinal mode, and the shear mode, the corresponding elastic constants for the three modes are c_{11}, c_{33}, and c_{55} respectively. Therefore, the electromechanical coupling coefficients of the three modes are as follows:

$$k_{31} = k_{32} = e_{31}/\sqrt{c_{11}^{\mathrm{E}}\varepsilon_3^{\mathrm{S}}}, \tag{17a}$$

$$k_{33} = e_{33}/\sqrt{c_{33}^{\mathrm{E}}\varepsilon_3^{\mathrm{S}}}, \tag{17b}$$

$$k_{15} = k_{24} = e_{15}/\sqrt{c_{55}^{\mathrm{E}}\varepsilon_1^{\mathrm{S}}}, \tag{17c}$$

respectively. By substituting Eqs. (17a)–(17b) into Eq. (16) separately, the elastic constants of the three modes when the piezoelectric plate is shunted to negative capacitance can be obtained as follows:

$$c_{11}^{\mathrm{SH}} = c_{11}^{\mathrm{E}}\left(1 + k_{31}^2\eta_3^{\mathrm{SH}}\right) = c_{11}^{\mathrm{E}}\left(1 + k_{31}^2\frac{C_{\mathrm{p}3}^{\mathrm{S}}}{C_{\mathrm{p}3}^{\mathrm{S}} - C_{x3}}\right), \tag{18a}$$

$$c_{33}^{\mathrm{SH}} = c_{33}^{\mathrm{E}}\left(1 + k_{33}^2\eta_3^{\mathrm{SH}}\right) = c_{33}^{\mathrm{E}}\left(1 + k_{33}^2\frac{C_{\mathrm{p}3}^{\mathrm{S}}}{C_{\mathrm{p}3}^{\mathrm{S}} - C_{x3}}\right), \tag{18b}$$

$$c_{55}^{\mathrm{SH}} = c_{55}^{\mathrm{E}}\left(1 + k_{15}^2\eta_1^{\mathrm{SH}}\right) = c_{55}^{\mathrm{E}}\left(1 + k_{15}^2\frac{C_{\mathrm{p}1}^{\mathrm{S}}}{C_{\mathrm{p}1}^{\mathrm{S}} - C_{x1}}\right). \tag{18c}$$

From Eqs. (18a)–(18c), it can be seen that the elastic constants of a piezoelectric plate shunted to a negative capacitor are determined by the value of the negative capacitance, the electromechanical coupling coefficient and the elastic constants of the piezoelectric material in short-circuit state. When the shunted circuit is in an open-circuit state, i.e., $C_x = 0$ and $\eta^{\mathrm{SH}} = 1$, the expressions in Eqs. (18a)–(18c) become:

$$c_{11}^{\mathrm{D}} = c_{11}^{\mathrm{E}}\left(1 + k_{31}^2\right), \tag{19a}$$

$$c_{33}^{\mathrm{D}} = c_{33}^{\mathrm{E}}\left(1 + k_{33}^2\right), \tag{19b}$$

$$c_{55}^{\mathrm{D}} = c_{55}^{\mathrm{E}}\left(1 + k_{15}^2\right), \tag{19c}$$

which are the normal relationships between the elastic constants in short-circuit state and that in open-circuit state.

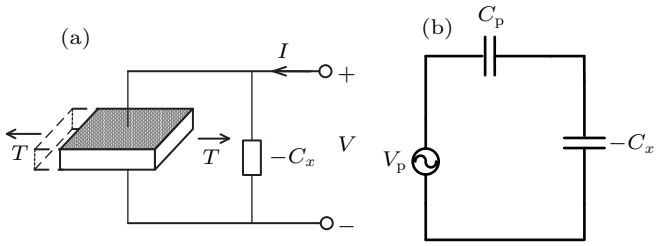


Fig. 2. Piezoelectric plate shunted to a negative capacitor: (a) physical model, (b) corresponding low-frequency equivalent circuit.

Taking piezoelectric material PZT-5A for example, elastic constants in Eqs. (18a)–(18c) are calculated and analyzed below. In order to normalize the influence of cross sectional area of the piezoelectric plate, the ratio of the value of the negative capacitor C_x to cross sectional area of the piezoelectric plate A is defined as the shunt capacitance ratio (SCR), i.e., $\mathrm{SCR} = C_x/A$, whose unit is F/m^2. According to Eqs. (18a)–(18c), with increase of the absolute value of the negative capacitance, the changes of elastic constants c_{11}, c_{33} and c_{55} of the shunted piezoelectric plate are calculated and illustrated in Figs. 3(a)–3(c), respectively. It can be seen that with the increase of the value of SCR, each of c_{11}, c_{33}, and c_{55} first increases monotonically to a positive maximum ($+\infty$ theoretically) from its initial value, i.e., c_{11}^{D}, c_{33}^{D}, and c_{55}^{D}, after an instantly reverse jump to a negative maximum ($-\infty$ theoretically), then monotonically increase to its final values, i.e., c_{11}^{E}, c_{33}^{E}, and c_{55}^{E}, respectively.

Based on Eqs. (18a)–(18c), the following relations can be found:

$$\text{if} \quad -1 < \frac{C_{\mathrm{p}3}}{-C_{x3}} < -\frac{1}{1 + k_{31}^2}, \quad \text{then} \quad c_{11}^{\mathrm{SH}} < 0; \tag{20a}$$

$$\text{if} \quad -1 < \frac{C_{\mathrm{p}3}}{-C_{x3}} < -\frac{1}{1 + k_{33}^2}, \quad \text{then} \quad c_{33}^{\mathrm{SH}} < 0; \tag{20b}$$

$$\text{if} \quad -1 < \frac{C_{\mathrm{p}1}}{-C_{x1}} < -\frac{1}{1 + k_{15}^2}, \quad \text{then} \quad c_{55}^{\mathrm{SH}} < 0. \tag{20c}$$

The conclusion in Eq. (20b) is the same as that in Eq. (4), which means that the structure is unstable if negative capacitance is improperly tuned. Equations (20a)–(20c) show that if

the value of negative capacitance is within whichever range of Eqs. (20a)–(20c), the corresponding elastic constant of piezoelectric plate will be lower than zero, which is not meaningful.

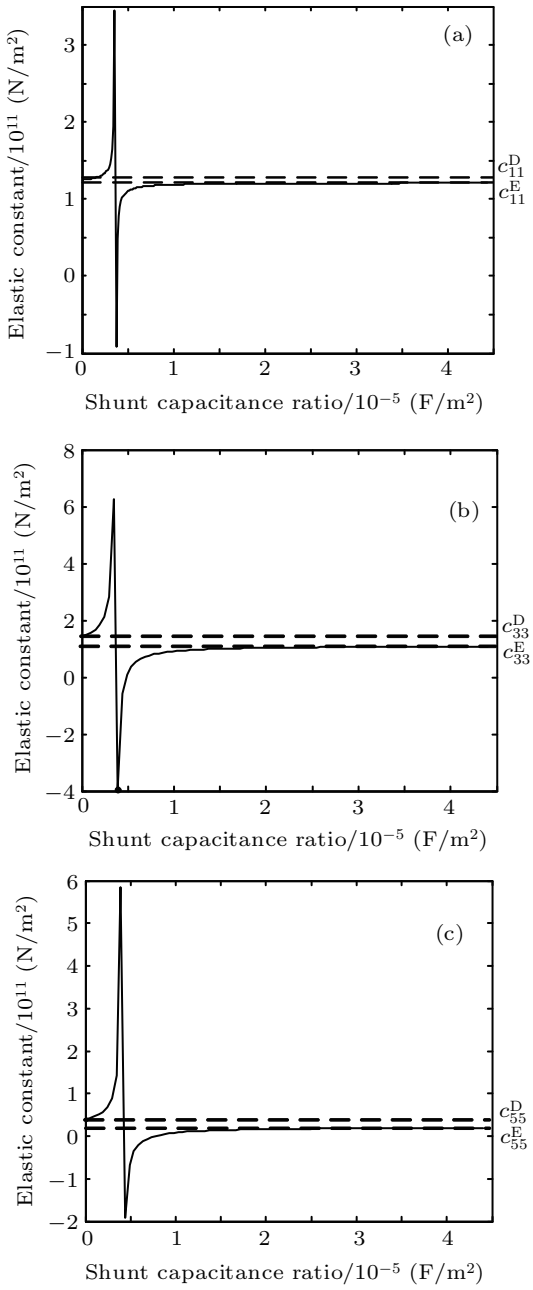


Fig. 3. Plots of elastic constants: (a) c_{11}, (b) c_{33}, and (c) c_{55} versus SCR.

3. Experiment verification

In order to verify the theoretical conclusions in Section 2, in this section, we investigate the variations of elastic constants of piezoelectric materials with shunt negative capacitance experimentally. Considering that the changes of elastic constants may be very small and easily submerged by measurement errors of direct mechanical test method, the indirect method[24] should be adopted in this paper, with which the variation of the elastic constants can be indirectly tested through observing the shift of resonant frequency of a mechanical resonator. In the design of experiment setup, the piezoelectric resonator should satisfy the following requirements. First, the measurement loop and the shunt circuit should be electrically isolated from each other to eliminate the directly electrical effect of the shunt circuit on the test loop, thereby ensuring that the shift of resonant frequency is purely caused by the change of the elastic constants. Thus the single resonator measurement method[26] is not applicable. Second, the mechanical system should be resonant at a frequency far below the natural frequency of the piezoelectric plate to avoid influencing the resonant peak of piezoelectric plate itself and make the piezoelectric plate work at a pseudo electrostatic state.

3.1. Experiment setup for c_{55} test

Since three elastic constants have the relationships similar to each other in the presence of the shunt negative capacitance, as shown in Eqs. (18a)–(18c), the measurement of c_{55} is taken as an example to verify the theoretical results in this paper. The thickness-shear mode (TSM) electro–mechanical resonant system in Ref. [24] is adopted to measure the change of the elastic constant c_{55} of piezoelectric plate with shunt negative capacitance. The scheme of experimental setup is shown in Fig. 4(a), including a TSM resonator, a shunt negative capacitance circuit, and an impedance analyzer. The TSM resonator is composed of two identical shear-mode piezoelectric ceramic plates a and b and a mass block m. Pure tungsten is chosen as the material of the mass block due to its high density to make the mass block close to a lumped-parameter element and the system close to an ideal spring oscillator. The experimental prototype of TSM resonator is shown in Fig. 4(b).

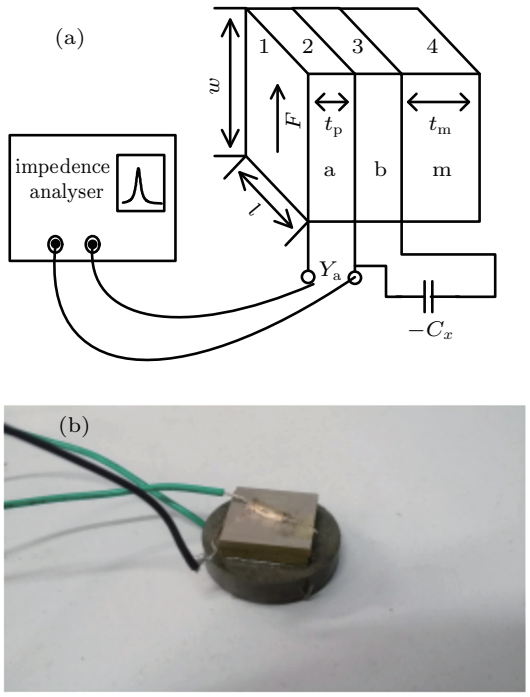


Fig. 4. (color online) (a) Scheme of experiment setup for c_{55} test. (b) Experimental prototype of the TSM resonator.

3.2. Realization of negative capacitance

Since the negative capacitance value needed in the experiments ranges from zero to infinite (large enough), the stable boundary of a single negative capacitance circuit is broken. Therefore, two kinds of negative capacitance circuits are realized in the experiments, which are demarcated by the value of the inner capacitance of piezoelectric plates.

One of the common negative capacitance shunt circuits is shown in Fig. 5(a). The non-inverting $(+)$ and inverting $(-)$ voltages of the operational amplifier (OA), i.e. V_{in}^{+} and V_{in}^{-}, are written, respectively, as

$$V_{\text{in}}^{-} = \frac{\frac{1}{\text{j}\omega C_{\text{p}}}}{R_1 + \frac{1}{\text{j}\omega C_{\text{p}}}} V_{\text{out}}, \tag{21a}$$

$$V_{\text{in}}^{+} = \frac{\frac{1}{\text{j}\omega C_x}}{R_2 + \frac{1}{\text{j}\omega C_x}} V_{\text{out}}. \tag{21b}$$

A negative capacitance C is obtained to be

$$C = -\frac{R_1}{R_2} C_x. \tag{22}$$

Usually, assume $R_1 = R_2$ to ensure the accuracy of the negative capacitance, then $C = -C_x$ will be obtained. The stable condition of the circuit (negative feedback) is

$$\text{d}\left(V_{\text{in}}^{+} - V_{\text{in}}^{-}\right)/\text{d}V_{\text{out}} < 0. \tag{23}$$

Combining Eqs. (21) with Eqs. (22) and (23), it is found that when $R_1 = R_2$, the stability condition is $|C| > C_{\text{p}}$.

Obviously, if the needed value of negative capacitance $|C|$ is smaller than C_{p}, the circuit in Fig. 5(a) will be instable, other realization circuit of negative capacitance should be considered. Figure 5(b) shows another type of negative capacitance circuit. Like the stability analysis made above, it can be found that the stability condition in Fig. 5(b) is $|C| < C_{\text{p}}$, which is contrary to Fig. 5(a).

Therefore, in experiment, when the needed value of negative capacitance $|C|$ is larger than the inner capacitance of piezoelectric plate C_{p}, the circuit in Fig. 5(a) is adopted. While for $|C| < C_{\text{p}}$, the circuit in Fig. 5(b) is employed.

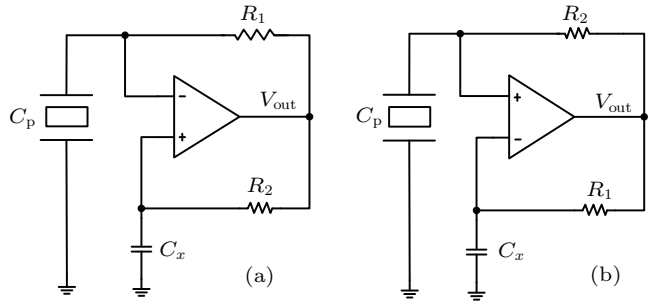


Fig. 5. The realization circuits of negative capacitance in the cases of (a) $|C| > C_{\text{p}}$ and (b) $|C| < C_{\text{p}}$.

In both circuits, the operational amplifier is Burr–Brown OPA552, which has the properties of high voltage, high current and wide bandwidth, and $R_1 = R_2 = 10$ kΩ.

3.3. Electrical conductance of TSM resonator

The conductance of the TSM resonator in Fig. 4(a) can be analyzed theoretically with Mason electro–mechanical equivalent circuit. The PZT-5A is chosen as the material of piezoelectric plates a, b in the calculation. The material parameters are shown in Table 1. The dimension parameters of resonant system in Fig. 4(a) are set to be $l = w = 1000$ mm to simulate the infinite boundary condition. Besides, $t_{\text{p}} = 2$ mm, and $t_{\text{m}} = 3$ mm.

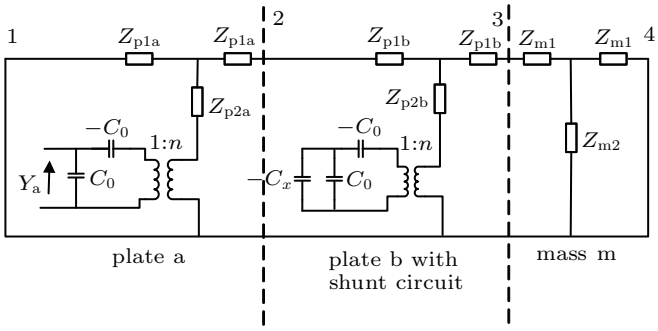


Fig. 6. Electro-mechanical equivalent circuit of TSM resonant system.[24]

Table 1. Parameters of piezoelectric ceramics, mass block and epoxy resin.

The piezoelectric ceramics PZT-5A											
Density/(kg/m^3)	Elastic constant/10^{10} (N/m^2)					Relative dielectric constant		Piezoelectric stress constant/(C/m^2)			Mechanical quality factor
ρ_{p}	c_{11}^{E}	c_{12}^{E}	c_{13}^{E}	c_{33}^{E}	c_{44}^{E}	$\varepsilon_{11}^{\text{S}}/\varepsilon_0$	$\varepsilon_{33}^{\text{S}}/\varepsilon_0$	e_{31}	e_{33}	e_{15}	Q_{m}^{D}
7500	12.1	7.54	7.52	11.1	2.11	916	830	–5.4	15.8	12.3	75
	c_{11}^{D}	c_{12}^{D}	c_{13}^{D}	c_{33}^{D}	c_{44}^{D}						
	12.6	8.09	6.52	14.7	3.97						
The mass block (tungsten)											
Density/(kg/m^3)	Young modulus/10^{10} (N/m^2)							Poisson's radio			
19100	35.4							0.35			
The epoxy resin											
Density/(kg/m^3)	Young modulus/10^{10} (N/m^2)					Poisson's radio		Damping factor			
1250	0.36					0.35		0.17			

Figure 6 shows the electro–mechanical equivalent circuit of the TSM resonant system. With plate b shunted to negative capacitance circuits, the electrical admittance Y_a of the system calculated from the two electrodes of plate a is derived from Fig. 6 as follows:[24]

$$Y_a = \frac{1}{\left(\frac{\left(Z_{m1}//Z_{m2}+Z_{m1}+Z_{p1b}\right)//\left(n^2\left(\left(-\frac{1}{j\omega C_x}\right)//\frac{1}{j\omega C_0}-\frac{1}{j\omega C_0}\right)+Z_{p2b}\right)+Z_{p1b}+Z_{p1a}}{n^2}//Z_{p1a}+Z_{p2a}-\frac{1}{j\omega C_0}\right)//\frac{1}{j\omega C_0}}, \quad (24)$$

where $Z_x = -1/j\omega C_x$ and C_x is the absolute capacitance value of the negative capacitance shunt circuit, and

$$Z_{p1a} = j\rho_p c_p^{open} S_p \tan\left(k_p^{open} t_p/2\right), \quad (25a)$$

$$Z_{p2a} = \rho_p c_p^{open} S_p/\left(j\sin\left(k_p^{open} t_p\right)\right), \quad (25b)$$

$$Z_{p1b} = j\rho_p c_p S_p \tan\left(k_p t_p/2\right), \quad (25c)$$

$$Z_{p2b} = \rho_p c_p S_p/\left(j\sin\left(k_p t_p\right)\right), \quad (25d)$$

$$Z_{m1} = j\rho_m c_m S_m \tan\left(k_m t_m/2\right), \quad (25e)$$

$$Z_{m2} = \rho_m c_m S_m/\left(j\sin\left(k_m t_m\right)\right). \quad (25f)$$

In Eq. (25), the subscripts 'p' and 'm' represent the piezoelectric plate and the mass block respectively. Correspondingly, ρ_p and ρ_m are their densities, S_p and S_m are their areas, t_p and t_m are their thickness values. Besides, $c_p^{open} = \sqrt{c_{55}^D/\rho_p}$ and $c_p = \sqrt{c_{55}/\rho_p}$ are the transverse wave velocities of piezoelectric ceramics in open state and shunted to circuits respectively, and thus $k_p^{open} = \omega/c_p^{open}$ and $k_p = \omega/c_p$ are the corresponding wave numbers. Moreover, c_m and $k_m = \omega/c_m$ are the transverse velocity and wave number of the mass block m, respectively. For the plates a and b, $C_0 = S_p\varepsilon_{11}^S/t_p$ is the inherent capacitance and $n = S_p h_{15}\varepsilon_{11}^S/t_p$ is the electromechanical conversion factor, in which ε_{11}^S is the dielectric constant and h_{15} is the shear-mode piezoelectric constant.

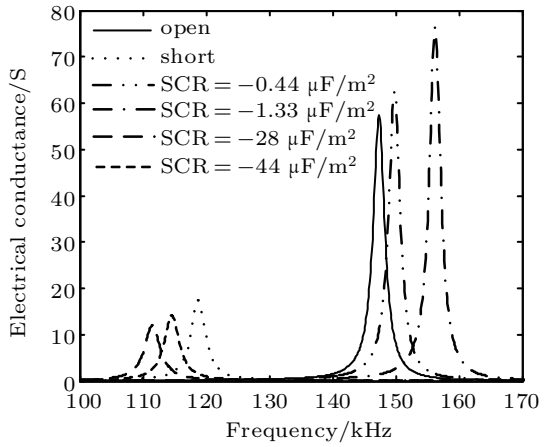


Fig. 7. Plots of electrical conductance of the system versus frequency, calculated from the two electrodes of plate a by equivalent circuit method with b shunted to negative capacitance.

With negative capacitance connected to plate b, the resonant frequency of the TSM resonator will shift. Figure 7 shows several conductance curves with different negative capacitance values connected to plate b, which are calculated from Eq. (24).

3.4. Theoretical prediction of relationships from conductance curves

The relationship between the elastic constant c_{55} and the shunt negative capacitance is not intuitive in Eq. (24). However, the physical process is known that the elastic constant c_{55} changes with shunt negative capacitance, which results in the shift of the resonant frequency of the TSM resonator. Thus through the observation of the shift of the resonant frequency of the TSM resonator, the variation of elastic constant c_{55} with the shunt negative capacitance can be indirectly obtained. The process can be resolved as three steps:

Step 1 Keep the plate b in an open-circuit state, i.e., no negative capacitance is connected, but change its elastic constant c_{55} numerically to observe the shift of the resonant frequency of the TSM resonator with the variation of c_{55}. As done in Ref. [24], c_{55} in Eq. (24) can be substituted with a complex number $c_{55} = c_{55r} + jc_{55i}$, where the subscripts 'r' and 'i' represent the real and the imagine parts, corresponding to elastic constant and damping factor respectively. Because the change range of the elastic constant c_{55r} induced by the negative capacitance shunt circuit is excessively wide, the conclusion in Ref. [24] that $\Delta c_{55r}/c_{55r}^D$ changes linearly with $\Delta f_r/f_r^D$ is inapplicable. The relationship between the elastic constant c_{55r} and the resonant frequency of the TSM resonator in the whole range is recalculated and obtained based on Eq. (24), which is shown in Fig. 8(a);

Step 2 Keep c_{55} in Eq. (24) constant, i.e., c_{55}^D, but change the value of negative capacitance to observe the shift of the resonant frequency of the TSM resonator with the variation of the value of negative capacitance. The relationship between the shunt negative capacitance $-C_x$ and the resonant frequency of the TSM resonator is shown in Fig. 8(b);

Step 3 Make the above two cases equivalent to each other to obtain the relationship between the elastic constant c_{55r} and the shunt negative capacitance through point mapping method, since the relationships in Fig. 8(a) and Fig. 8(b) are both single-valued curves. The relationship between the elastic constant c_{55r} and the negative capacitance is achieved and

shown in Fig. 8(c).

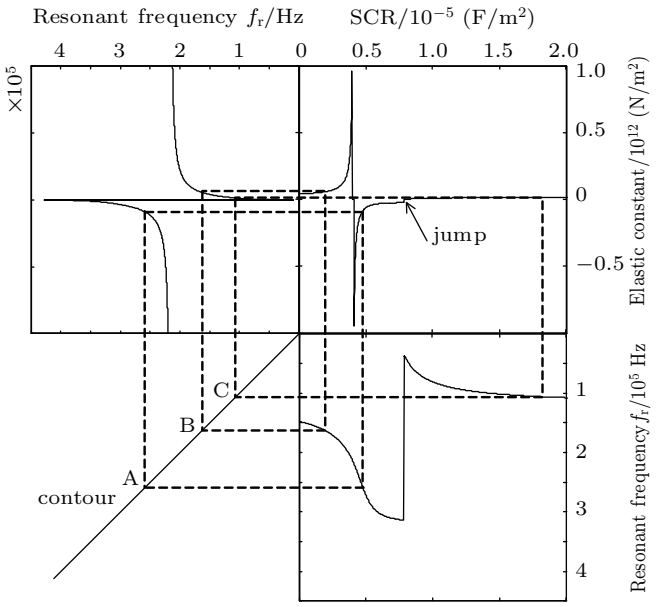


Fig. 8. Relationships between (a) resonant frequency f_r and elastic constant c_{55r}, (b) resonant frequency f_r and SCR, and (c) elastic constant c_{55r} and SCR.

The curves in Fig. 8 are divided into three parts. In the first part, the ranges of the elastic constant, SCR and the resonant frequency are $(4 \sim 96) \times 10^{10}$ N/m^2, $1.1 \times 10^{-7} \sim 3.97 \times 10^{-6}$ F/m^2, and 148 kHz $\sim$ 212 kHz respectively. The dashed rectangle B is a representative map of this part. In the second part, the ranges of the elastic constant, SCR and the resonant frequency are $(-94 \sim -2.11) \times 10^{10}$ N/m^2, $(3.97 \sim 7.85) \times 10^{-6}$ F/m^2, and 212 kHz$\sim$ 314 kHz respectively. The dashed rectangle A is a representative map in this part. In the third part, the ranges of the elastic constant, SCR and the resonant frequency are $(0.18 \sim 2) \times 10^{10}$ N/m^2, $7.86 \times 10^{-6} \sim 5 \times 10^{-5}$ F/m^2, and 37.2 kHz$\sim$ 115 kHz respectively. The dashed rectangle C is a representative map in this part.

From Fig. 8, it is seen that with the increase of SCR, the resonant frequency of the system first increases from its open-circuit f_r^D to a maximum value, after an instantly reverse jump to the minimum, then continuously increases to its short-circuit f_r^E. Meanwhile, with the increase of SCR, c_{55r} first increases from its open-circuit value c_{55r}^D to a maximum value, after an instantly reverse jump to the negative maximum, then continuously increases to its final value, the elastic constant under constant electrical field, i.e., c_{55r}^E, correspondingly. The conclusion is the same as the result obtained by theoretical analysis with the piezoelectric constitutive law in Section 2.

By comparing the ranges of resonant frequency in Fig. 8(a) and Fig. 8(b), it is found that the range of resonant frequency from 313 kHz to 419 kHz can be achieved by changing the elastic constant c_{55r} in Fig. 8(a), but it cannot be reached by changing the negative capacitance value in Fig. 8(b), where the resonant frequency curve becomes flat near 313 kHz. In other words, the corresponding range of the elastic constant c_{55r} from -2.11×10^{10} N/m^2 to 0 cannot be achieved by changing the negative capacitance. This is because the elastic constant of the two piezoelectric plates in series will be lower than zero when the elastic constant c_{55r} falls in a range of -2.11×10^{10} N/m^2 to 0. This will result in the instability of the system. It is also the reason for the jump in Fig. 8(c).

3.5. Experimental tests

The experimental prototype of TSM resonator was fabricated as shown in Fig. 4(b). The thickness of each piezoelectric plate was $t_p = 2$ mm, corresponding to a natural frequency of 1 MHz. The thickness of the mass block was $t_m = 3$ mm. Because of limitation of the poling length, in practice the lateral dimensions of the piezoelectric plates were machined into $l = w = 15$ mm, much smaller than those used in the theoretical analysis in Subsection 3.3. In fact, the shear mode vibration is less affected by the lateral boundary condition than the thickness mode. If the length-to-thickness ratio of the piezoelectric plate is not too small, the lateral boundary effect on the resonant frequency of the system is negligible. Our simulation reveals that a length-to-thickness ratio greater than 2 can satisfy the infinite lateral condition requirement approximately.

In the experiments, with two negative capacitance circuits, a series of values of negative capacitance was realized. The conductance curves of the prototype system in Fig. 4(b) were tested from two ends of plate a by an impedance analyzer, with piezoelectric plate b shunted to negative capacitance circuit. Some results are shown in Fig. 9. In comparison with Fig. 7, it is seen that with the variation of SCR, the changes of conductance curves of the TSM resonator show similar variation tendencies. However, all the resonant frequencies are lower than the predicted ones in Subsection 3.3. This is because the epoxy resin bonding layers exist, respectively, between plates a and b, and between plate b and mass block m of the prototype sample, which are connected in series with the elastic piezoelectric plates. Besides, the bandwidths of the experimental conductance peaks are broadened accordingly, in comparison with the theoretical predicted ones. This is caused by the epoxy resin layers too, which have lager damping factor than piezoelectric plates.

By picking up the peak position of conductance of plate a, the relationship between the resonant frequency of the TSM resonator and the negative capacitance is also measured, and shown in Fig. 10. It is seen that with the increase of SCR, the change of the resonant frequency has a similar variation tendency to that of the theoretical analysis with Mason equivalent

circuit. It means the elastic constant $c_{55\mathrm{r}}$ indeed has a similar variation to that of the resonant frequency, as the theoretical analyses demonstrated in Section 2 and Subsection 3.4.

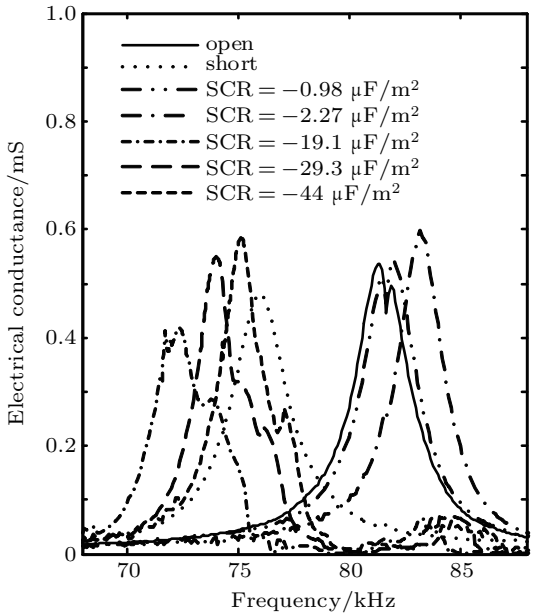


Fig. 9. Electrical conductance of the system measured from the two electrodes of plate a experimentally, with b shunted to negative capacitance.

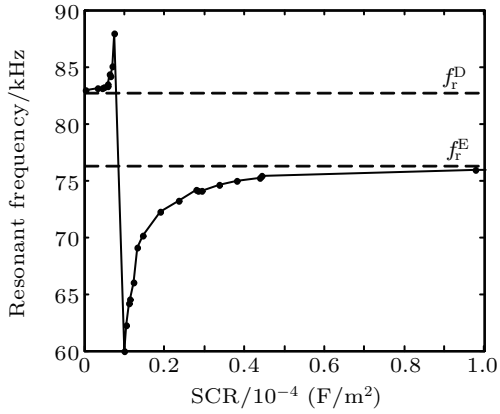


Fig. 10. Variation of resonant frequency with SCR, measured in experiment.

4. Discussion

Most vibration suppression or sound absorption systems require their negative capacitances to be near to the inner capacitances of piezoelectric ceramics to achieve the optimal performances.[21–23] However, based on the theoretical results extracted from Fig. 3(c) and Fig. 8(c), it is found that a singular point of elastic constants occurs just at the position of SCR corresponding to the inner capacitance under constant strain $C_{\mathrm{p}}^{\mathrm{S}}$ of the piezoelectric plate. The experimental results also verify the phenomenon. It means that the elastic constants will take singular values in this case. Therefore, the optimal condition, i.e., the negative capacitance equals the inner capacitance, which is just the stability margins of the shunted systems, cannot be satisfied in practice. In fact, even a suboptimal condition, i.e., a negative capacitance close to the inner capacitance, is not applicable either. Since the inner capacitance of a piezoelectric material is easily affected by environmental factors like temperature, a slight change of inner capacitance may also lead to the instability of the system. Furthermore, from Figs. 3(c) and 8(c), it is found that the range of SCR having significant influence on elastic constants is very narrow. If the negative capacitance shunted systems is chosen and works at a slow change region of elastic constants to ensure the stability, it will have no significant improvement in the performance. This may be a good explanation for why the negative capacitance technique cannot behave well in practical applications such as vibration suppression, sound absorption, etc.

5. Conclusions

In this paper, we investigate the influences of shunt negative capacitance on elastic constants of piezoelectric material of the transverse mode, the longitudinal mode and the shear mode, i.e., c_{11}, c_{33}, and c_{55}, respectively. Through the theoretical analyses with the piezoelectric constitutive equations, the relationships between the shunt negative capacitance and the elastic constants are obtained, showing the singular variation properties of the elastic constants on condition that the negative capacitance equals the inner capacitance. The thickness-shear mode elastic constant c_{55} is taken as an example to be studied experimentally with a TSM resonator. The experimental results show a variation tendency similar to those obtained from the theoretical analyses with using the constitutive equation and the Mason equivalent circuit methods. The results reveal the inner cause of instability of the piezoelectric damping system shunted to negative capacitance. Besides, the results show that the effective range of the negative capacitance is very narrow, while most of the negative capacitance region has little influence on the elastic constants. This is also a good explanation for why most shunt damping systems each with shunt negative capacitance show no significant improvement of performance in practical applications.

References

[1] Forward R L 1979 *Appl. Opt.* **18** 690
[2] Hagood N W and von Flotow A 1991 *J. Sound Vib.* **146** 243
[3] Becker J, Fein O, Maess M and Gaul L 2006 *Comput. Struct.* **84** 2340
[4] Thomas O, Ducarne J and Deü J F 2012 *Smart Mater. Struct.* **21** 015008
[5] Sun Y, Li Z H, Huang A G and Li Q H 2015 *J. Sound Vib.* **355** 19
[6] Zhang J M, Chang W, Varadan V K and Varadan V V 2001 *Smart Mater. Struct.* **10** 414
[7] Ahmadian M and Jeric K M 2001 *J. Sound Vib.* **243** 347
[8] Guyomar D, Richard T and Richard C 2008 *J. Intell. Mater. Syst. Struct.* **19** 791

[9] Kim J S, Jeong U C, Seo J H, Kim Y D, Lee O D and Oh J E 2015 *Sensor. Actuat. A-Phys.* **233** 330
[10] Kim J and Lee J K 2002 *J. Acoust. Soc. Am.* **112** 990
[11] Chen S B, Wen J H, Wang G and Wen X S 2013 *Chin. Phys. B* **22** 074301
[12] Hollkamp J J 1994 *J. Intell. Mater. Syst. Struct.* **5** 49
[13] Wu S 1998 *Proceedings of SPIE* **3327** 159
[14] Behrens S, Moheimani S O R and Fleming A J 2003 *J. Sound Vib.* **266** 929
[15] Riordan R H S 1967 *Electron. Lett.* **3** 50
[16] Behrens S, Fleming A J and Moheimani S O R 2003 *Smart Mater. Struct.* **12** 18
[17] Behrens S, Fleming A J and Moheimani S O R 2001 *Proc. SPIE* **4331** 239
[18] Fukada E, Date M, Kimura K, Okubo T, Kodama H, Mokry P and Yamamoto K 2004 *IEEE Trans. Dielectr. Electr. Insul.* **11** 328
[19] Yu L G, Li Z H and Ma L L 2012 *Acta Phys. Sin.* **61** 024301 (in Chinese)
[20] Neubauer M, Oleskiewicz R, Popp K and Krzyzynski T 2006 *J. Sound Vib.* **298** 84
[21] de Marneffe B and Preumont A 2008 *Smart Mater. Struct.* **17** 035015
[22] Han X, Neubauer M and Wallaschek J 2013 *J. Sound Vib.* **332** 7
[23] Neubauer M and Wallaschek J 2009 *IEEE/ASME International Conference on AIM* 1100
[24] Hu J Y, Li Z H, Sun Y and Li Q H 2016 *Chin. Phys. B.* **25** 127701
[25] Luan G D, Zhang J D and Wang R Q 2005 *Piezoelectric Transducers and Arrays* (Beijing: Peking University Press) pp. 26–72
[26] Hafner E 1969 *Proc. IEEE* **57** 179